

Influence of space charged particles on satellite optical communication system

RUI HOU*, SHANGHONG ZHAO, JIE XU, JILI WU, YONGJUN LI,
SHENGBAO ZHAN, LEI SHI, SHAOQIANG FANG

Telecommunication Engineering Institute, Air Force Engineering University, Xi'an 710077, China

*Corresponding author: houruirachel@yahoo.com.cn

Although research of satellite optical communication system has been carried out for many years, there is scarce literature to comprehensively analyze the influence of space environment on satellite optical communication system. Different kinds of particles and fields exist in the space environment, including high energy charged particles, solar radiation, plasma environment, space fragment, *etc.* The influence of space charged particles on satellite optical communication system was investigated in detail, which mainly related to single event upset (SEU), total dose effect and plasma environment. For SEU analysis the relation between single proton upset rate and satellite orbit was analyzed in detail. The reliability index of equipment based on SEU was proposed, the numerical calculation results have proved that the SEU effect was relatively less and corresponded to higher reliability of SRAM/MOS equipment under lower orbit altitude and inclination. For plasma environment analysis there is no obvious influence of plasma on laser signal transmission. But charging and discharging processes on satellite surface would lead to the malfunction of satellite communication system. The influence of charged particles and its related plasma on satellite optical communication system was investigated, which would be helpful for the design and the improvement of performance of satellite optical communication system.

Keywords: satellite optical communication, charged particle, single event upset, plasma.

1. Introduction

The satellite communication technique based on microwave could not meet the requirement of space information transmission. The satellite optical communication system has advantages compared with microwave communication system [1], it has larger information capacity, good direction, it is smaller and lighter, and so on. It has become a possible information transmission scenario in the space. A great deal of literature and experiments have been developed to explore and improve the satellite optical communication system, which mainly focus on the improvement of BER (bit error ratio) system. The transmission medium was considered to be free space. Actually, there are different kinds of particles and fields in the space environment [2],

including high energy charged particles, solar radiation, plasma environment and space fragment. The laser communication terminal is a complex integrative equipment, which has higher requirements of satellite optical communication system compared with microwave's. According to statistics, nearly 40% of satellite malfunctions were induced by space environment. Although the research of satellite optical communication system had been carried out for many years, there was scarce literature to comprehensively analyze the influence of space environment on satellite optical communication system, which we believed to be interesting and important. It would be helpful for the design and the performance and stability of satellite optical communication system. The charged particles are common in space, which were considered to be first investigated.

2. Single event upset effect

2.1. SEU prediction

The single event upset (SEU) is caused by a single particle deposition, which results in "soft error". The high energy charged particles in space (proton, heavy ion, and neutron) shorten micro-electronic equipment, and produce large numbers of electron-hole pairs inner equipment. The instantaneous upset of electronic equipment would appear under the action of inner electric field equipment. It induces large scale and super-large scale electronic circuits causing mistakes or temporary invalidation. Single event upset rate is defined as the SEU occurrences in unit time, being generally represented by 1/(bit·day).

The research on SEU is always performed through satellite experiment and ground simulation. The latter is completed by a heavy ion accelerator, which is convenient to be realized. There are different methods to complete SEU prediction, in which some errors exist. Two methods with less errors, differential energy spectrum and figure of merit (FOM) have been used to evaluate SEU. Further, the effects of SEU on the reliability of satellite optical communication system are discussed.

2.1.1. SEU prediction through differential energy spectrum

The satellite is always shielded by an aluminum shell. The differential energy spectrum [3] of inner particles $f(E)$ can be expressed as:

$$f(E) = f'(E') \frac{S(E')}{S(E)} \exp(-ct) \quad (1)$$

$$E' = R^{-1} [R(E) + t] \quad (2)$$

$$c = \frac{\eta(A^{1/3} + 8.6)^2}{27} \times 5 \times 10^{-26} \quad (3)$$

where $f'(E')$ is the differential energy spectrum of satellite surface ($\text{cm}^{-2}\cdot\text{d}^{-1}\cdot\text{MeV}^{-1}$); E is the particle energy inner satellite (MeV); $R(E)$ is the transmission distance of particle with energy E ; $S(E)$ is the held back energy of particle; A is the mass of particle; t is the thickness of aluminum shell; η is the Avogadro constant.

The SEU rate R_h (1/(bit-day)) could be expressed through linear energy transition (LET) spectrum and SEU cross-section area with different LET values

$$R_h = \int_0^{\infty} f_e(L) \sigma_0(L) dL \quad (4)$$

L is LET value of heavy ion ($\text{MeV}\cdot\text{cm}^2\cdot\text{mg}^{-1}$); $\sigma_0(L)$ is the SEU cross-section area of heavy ion; $f_e(L)$ is the equivalent differential energy spectrum [4] of heavy ion, which can be expressed as

$$f_e(L) = \frac{f(L)}{2\pi} \int_{\theta_c}^{\frac{\pi}{2}} \cos(\theta) d\Omega = \frac{f(L)}{2} \cos^2(\theta_c) =$$

$$= \begin{cases} \frac{f(L)}{2} \left(\frac{L}{L_0}\right)^2 & L \leq L_0 \\ \frac{f(L)}{2} & L > L_0 \end{cases} \quad (5)$$

$f(L)$ is the differential energy spectrum of heavy ion; L_0 is the LET threshold of SEU; the critical angle at which SEU occurs is $\theta_c = \arccos(L/L_0)$.

According to experimental results, the SEU rate [4] of proton R_p could be expressed as

$$R_p = \int_0^{\infty} \sigma_0 \left\{ 1 - \exp \left[- \left(\frac{L - L_0}{W} \right)^S \right] \right\} \varphi(L) dL \quad (6)$$

$$\varphi(L) = 2.4 \times 10^{-6} \times \int_0^{\infty} f(E_p) \left(0.134 + \frac{9}{E} \right) \exp \left[\left(0.134 + \frac{9}{E} \right) L \right] dE \quad (7)$$

where W and S are Weibull parameters; $\varphi(L)$ is the effective differential LET function of proton.

The final SEU rate, under the action of both proton and heavy ion, can be expressed as follows:

$$R = R_p + R_h \quad (8)$$

2.1.2. SEU prediction through FOM

The FOM method can also be used to predict SEU rate, which can be calculated as

$$R = R_p + R_h = (C_p + C_h) F = (C_p + C_h) \frac{\sigma_{hL}}{L_{0.25}^2} \quad (9)$$

where C_p and C_h are the orbit SEU coefficients of proton and heavy ion (upsets/(bit-day)); parameters F could be achieved through experimental results for heavy ion $\sigma_{hL}/L_{0.25}^2$; σ_{hL} is the SEU saturation cross-section (cm^2/bit); $L_{0.25}$ is the LET value corresponding to the 25% of SEU saturation cross-section, $L_{0.25} = L_0 + 0.288^{1/S} W$.

There are two kinds of equipment (enhanced and un-enhanced), which are characterized by the same shielding conditions. The SEU rate R_1 and parameter F_1 of equipment 1 can be calculated by differential energy spectrum method, then the SEU coefficient can be obtained from $C = R_1/F_1$. For equipment 2, the parameters σ_{hL} and $L_{0.25}$ are obtained, the parameter F_2 can be calculated. The SEU rate of some orbit can be calculated as $R_2 = CF_2$. For the satellites on the same orbit, the SEU coefficient changes with the shielding thickness. C_{t_1} is defined as the SEU coefficient of shielding thickness t_1 , C_{t_2} is the SEU coefficient of shielding thickness t_2 [5], then

$$C_{t_2} = 2C_{t_1} - 0.5 C_{t_1} \log(t) \quad (10)$$

T a b l e 1. Parameters of equipment.

Devices	Satellites	Type	L_0	W	S	σ_{hL}	F
			[MeV/mg/cm ²]			[$\mu\text{m}^2/\text{bit}$]	
HM6516	UOSAT-2	Hitachi, 16K CMOS SRAM	5	14	1.9	180	1.195×10^{-8}
2164	CRESS	MOS	0.487	4.95	1.42	170	2.62×10^{-7}

T a b l e 2. SEU rates of HM6516 on different orbits.

Orbits	SEU rate coefficient [upsets/(bit-day)]			SEU rate [1/(bit-day)]		
	C_p	C_H	C	R_p	R_H	R
Low Earth orbit (LEO) (500 km/52°)	103.31	3.62	106.93	1.23×10^{-6}	4.33×10^{-8}	2.09×10^{-6}
Sun synchronous orbit (870 km/98.9°)	436.16	38.96	475.12	5.21×10^{-6}	4.66×10^{-7}	5.68×10^{-6}
Geostationary Earth orbit (GEO) (35790 km/0°)	0.11	75.61	75.72	0.13×10^{-8}	9.04×10^{-7}	9.05×10^{-7}
High Earth orbit (HEO) (20000 km/63.4°)	0.10	113.19	113.29	1.195×10^{-9}	1.35×10^{-6}	1.35×10^{-6}
Highly elliptical orbit (200×36000 km/28.5°)	878.56	57.80	936.36	1.05×10^{-5}	6.91×10^{-7}	1.12×10^{-5}

2.2. SEU rate analysis

In the satellite optical communication system, SRAM and CMOS equipment saves important control bit, whose SEU-induced errors would lead to the malfunction of satellite optical communication system. According to some experimental results [6, 7], under the shielding of a 3.3 mm aluminum shell, the SRAM device HM6516 and MOS device 2164 on satellite have been discussed, whose parameters are listed in Tab. 1.

2.2.1. SEU rates of different orbits

According to the parameters from Tab. 1, the SEU rates of unenhanced HM6516 on different orbits are shown in Tab. 2.

It can be seen from Tab. 2 that the orbits of SEU induced by proton mainly include LEO, Sun synchronous orbit, and highly elliptical orbit; the orbits of SEU induced by heavy ion mainly include GEO and HEO.

2.2.2. SEU rate of LEO

Although the space radiation and flux of high energy proton and heavy ion are lower, the SEU of LEO is an important factor that affects the reliability of equipment on satellite. The MOS device 2164 was analyzed, the SEU rates on different orbits were calculated, as listed in Tab. 3. The typical altitudes of orbits were selected as 500 km and 1000 km, the proton SEU rates of different orbit inclinations were calculated, see Tab. 4.

It can be seen from Tabs. 3 and 4 that the SEU of proton increases with an increase in the orbit altitude; the SEU rate at 0° inclination increases much faster. For 500 km and 1000 km orbits the SEU rates reach maximum at 30° and 20°, respectively.

Table 3. Proton SEU rates of MOS 2164 at 0°, 30° and 60° inclinations.

Orbit altitude [km]	0°		30°		60°	
	C_p	R_p	C_p	R_p	C_p	R_p
200	—	—	0.1	2.62×10^{-8}	0.07	1.83×10^{-8}
300	—	—	2	5.24×10^{-7}	0.85	2.27×10^{-7}
400	—	—	10	2.62×10^{-6}	4.7	1.23×10^{-6}
500	—	—	40	1.05×10^{-5}	18	4.72×10^{-6}
600	0.01	2.62×10^{-9}	100	2.62×10^{-5}	42	1.10×10^{-5}
700	3.1	8.12×10^{-7}	200	5.24×10^{-5}	85	2.23×10^{-5}
800	72	1.89×10^{-6}	300	7.86×10^{-5}	143	3.75×10^{-5}
900	225	5.90×10^{-6}	420	1.10×10^{-4}	230	6.03×10^{-5}
1000	553	1.45×10^{-4}	690	1.81×10^{-4}	302	7.91×10^{-5}
1100	1000	2.62×10^{-4}	1000	2.62×10^{-4}	545	1.43×10^{-4}
1200	1600	4.19×10^{-4}	1500	3.93×10^{-4}	700	1.83×10^{-4}
1300	3000	7.86×10^{-4}	2000	5.24×10^{-4}	1000	2.62×10^{-4}
1400	3260	8.54×10^{-4}	3300	8.65×10^{-4}	4950	1.30×10^{-3}

T a b l e 4. Proton SEU rates of MOS 2164 at 500 km and 1000 km.

Orbit inclination [°]	500 km		1000 km	
	C_p	R_p	C_p	R_p
5	0.01	2.62×10^{-9}	580	1.52×10^{-4}
10	0.5	1.31×10^{-7}	600	1.57×10^{-4}
20	14	3.67×10^{-6}	730	1.91×10^{-4}
30	40	1.05×10^{-5}	620	1.62×10^{-4}
40	31	8.12×10^{-6}	500	1.31×10^{-4}
50	22	5.76×10^{-6}	410	1.07×10^{-4}
60	17	4.45×10^{-6}	330	8.65×10^{-5}
70	16	4.19×10^{-6}	300	7.86×10^{-5}
80	16	4.19×10^{-6}	280	7.34×10^{-5}
90	16	4.19×10^{-6}	260	6.81×10^{-5}

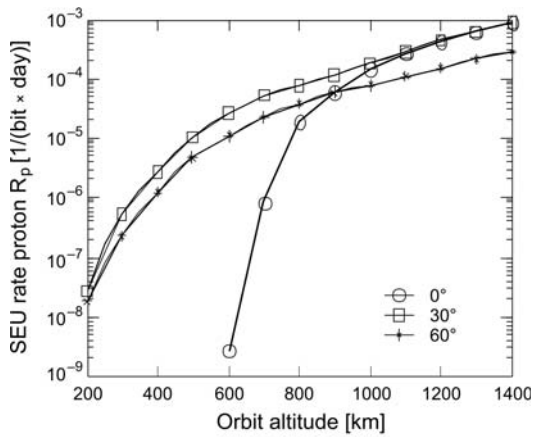


Fig. 1. Variations of SEU rate of proton with orbit altitude.

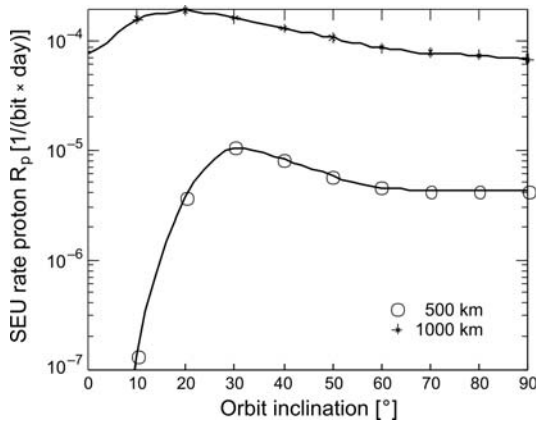


Fig. 2. Variations of SEU rate of proton with orbit inclination.

The numerical fit of discrete data in Tabs. 3 and 4 would directly present the variations of SEU, which are shown in Figs. 1 and 2. It can be seen from Fig. 1 that when orbit altitude changes from 200 km to 900 km, the SEU rate reaches its maximum at 30° inclination, the second maximum place is at 60°, the 0° inclination is minimum, but it changes fast. When the orbit altitude is higher than 1100 km, the SEU rate reaches maximum at the 0° inclination and minimum at 60° inclination. It can be seen from Fig. 2 that for a 500 km orbit, when the inclination is between 0° and 30°, the SEU rate of proton changes greatly; when the inclination is between 30° and 60°, the SEU rate varies slowly; when the inclination surpasses 60°, the SEU rate almost does not change. For a 1000 km orbit, when the inclination is between 0° and 20°, the SEU rate increases with an increase of orbit inclination; when the inclination is over 20°, the SEU rate decreases with an increase of orbit inclination.

2.3. Equipment reliability analysis

According to the long term measurements, the SEU is considered as a random event ξ , with the probability of SEU of a single memory bit being the Poisson distribution,

$$p(\xi = k) = \frac{\lambda^k}{k!} e^{-\lambda}, \quad k = 0, 1, 2, \dots \quad (11)$$

where k is the number of times that SEU happens ($k = 0$ represents the probability that no upset happens); $\lambda = RT$ is the mean value of SEU; $P_0 = e^{-RT}$.

The SEU reliability index of equipment P_R is defined as

$$P_R = 1 - e^{-RT} \quad (12)$$

For enhanced equipment P_R can be expressed as

$$R_r = fR_0 \quad (13)$$

$$P_R = 1 - e^{-TR_r} = 1 - e^{-TfR_0} \quad (14)$$

where T is the lifetime of satellite; f is a parameter related to the enhanced equipment. The relations between the SEU of LEO satellite and inclination and altitude through the lifetime of satellite are shown in Figs. 3 and 4.

3. Plasma environment

3.1. Plasma frequency

The plasma environment is also related to charged particles. The plasma frequency ω_p is determined by the density of free electrons in plasma. Collisions are caused by the movement of charged particles, therefore the electromagnetic wave would be

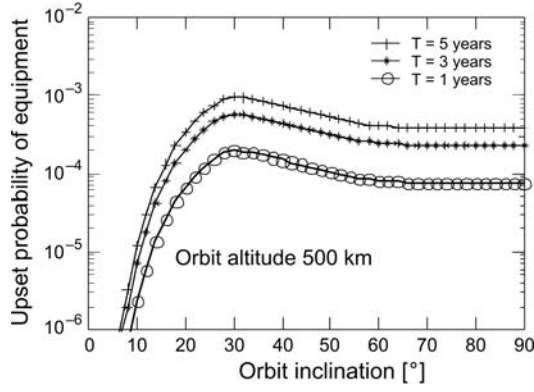


Fig. 3. Variations of upset probability of equipment with orbit inclination.

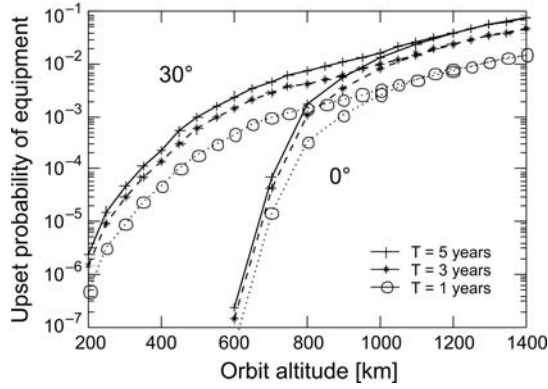


Fig. 4. Variations of upset probability of equipment with orbit altitude.

absorbed by plasma. When the frequency of incident wave $\omega > \omega_p$, it could transmit in the plasma; if $\omega < \omega_p$ the incident wave would be totally reflected.

Because the mass of positive ion is greatly larger than that of electron, here we only consider the movements of electrons. The density of electrons is N ; the mass of electron is m ; velocity is v ; charge quantity is e , then the movements of electrons satisfy

$$\frac{\partial N}{\partial t} + \Delta \cdot (Nv) = 0 \quad (15)$$

Because the magnetic force is much lower than electric force, which could be neglected [8], then

$$m \frac{dv}{dt} = m \left[\frac{\partial v}{\partial t} + (v \cdot \Delta)v \right] = -e E_i \quad (16)$$

The electric field of incident wave is $E_e = E_e(xe^{-j\omega t})$ and $j = j_0 e^{-j\omega t}$, then

$$j = i \frac{n_0 e^2}{m \omega} E_e = \sigma_c(\omega) E_e(\omega) \quad (17)$$

The electric conductivity $\sigma_c(\omega) = i[(n_0 e^2)/(m\omega)]$ is pure imaginary number, which shows a phase difference of $\pi/2$ between j and E_e . There is no energy attenuation, the average power is $\bar{P} = 0$. The complex dielectric constant is $\varepsilon' = \varepsilon + i[\sigma_c/\omega]$, then

$$\varepsilon' = \varepsilon_0 - \frac{n_0 e^2}{m\omega^2} = \varepsilon_0 \left(1 - \frac{n_0 e^2}{m\varepsilon_0 \omega^2} \right) = \varepsilon_0 \varepsilon_r' \quad (18)$$

It can be seen from Eq. (18) that the plasma frequency ω_p is determined by $[1 - n_0 e^2/m\varepsilon_0 \omega^2] = 0$, $\omega_p = n_0 e^2/m\varepsilon_0$. When the frequency of electromagnetic wave $\omega > \omega_p$, the real part of ε' is larger than 0, the incident wave could transmit into plasma and be used in satellite communication, except for some attenuation. When $\omega < \omega_p$, the incident wave is totally reflected at the interface between free space and plasma. For satellite optical communication system, whose frequency of laser signal is 10^{14} Hz or even much higher, and the plasma frequency is generally between 10^6 Hz and 10^7 Hz, therefore $\omega \gg \omega_p$, there would be no total reflection of laser signal.

3.2. Effects of plasma on laser signal transmission

The effects of plasma on electromagnetic wave will be used to analyze the effects of plasma on laser signal transmission. The transmission equation of electromagnetic wave in plasma [9] is

$$\nabla \times \nabla \times E = -\varepsilon_0 \mu_0 \tilde{\varepsilon}_r \frac{\partial^2 E}{\partial t^2} \quad (19)$$

Here, we only consider the interactions between plane wave and single layer plasma. Assume that the electromagnetic wave transmitted along z axis, so

$$E = E_0 \exp(j\omega t - \tilde{\gamma} z) \quad j \equiv \sqrt{-1} \quad (20)$$

where ω is the frequency of electromagnetic wave; $\tilde{\gamma}$ is the transmission constant; the dispersion relation of electromagnetic wave in plasma is

$$\tilde{\gamma}^2 = -\frac{\omega^2}{c^2} \tilde{\varepsilon}_r \quad (21)$$

where c is the light velocity. The transmission constant [10] of electromagnetic wave in plasma is

$$\tilde{\gamma} = j \frac{\omega}{c} \sqrt{\tilde{\varepsilon}_r} = \alpha + j\beta \quad (22)$$

where the real part α is attenuation coefficient; the imaginary part β is phase constant. In partially ionized plasma the density of neutral gas is greatly larger than that of plasma, therefore the collisions of electrons and plasma could be neglected. Besides,

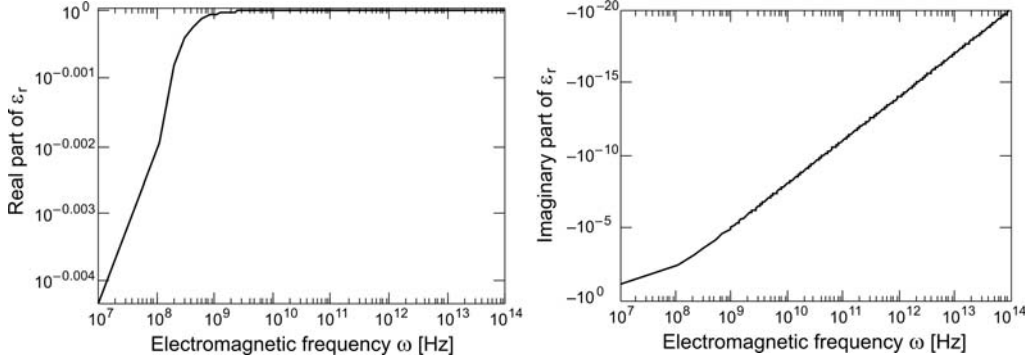


Fig. 5. Relation between dielectric constant and electromagnetic frequency.

the mass of ion is also greatly larger than that of electron, whose movement could be neglected, so

$$\tilde{\varepsilon}_r = 1 - \frac{\omega_p^2}{\omega^2 + \nu_{\text{en}}^2} - j \frac{\omega_p^2 \nu_{\text{en}} / \omega}{\omega^2 + \nu_{\text{en}}^2} \quad (23)$$

where ω_p is plasma frequency, $\omega_p = \sqrt{n_0 e^2 / m \varepsilon_0}$; ω is the frequency of electromagnetic wave; ν_{en} is the collision frequency between electrons and neutral gas. The plasma frequency is selected as $\omega_p = 10^7$ Hz, collision frequency $\nu_{\text{en}} = 10^8$ Hz; the relation between complex dielectric constant and frequency of electromagnetic wave is shown in Fig. 5.

The initial transmitting power of electromagnetic wave is assumed to be P_0 ; the power transmitted into plasma is P_i ; the power reflected by interface is P_r , and it satisfies

$$\frac{P_r}{P_0} = \left| \frac{1 - \sqrt{\tilde{\varepsilon}_r}}{1 + \sqrt{\tilde{\varepsilon}_r}} \right|^2 \quad (24)$$

The power transmitted into plasma is

$$P_i = P_0 - P_r \approx P_0 \quad (25)$$

The power that transmitted into plasma at the place z is

$$P(z) = P_0 \exp(-2\alpha z) \quad (26)$$

The thickness of plasma is d , the power of electromagnetic wave transmitted through plasma is

$$P_t = P_0 \exp(-2\alpha d) \quad (27)$$

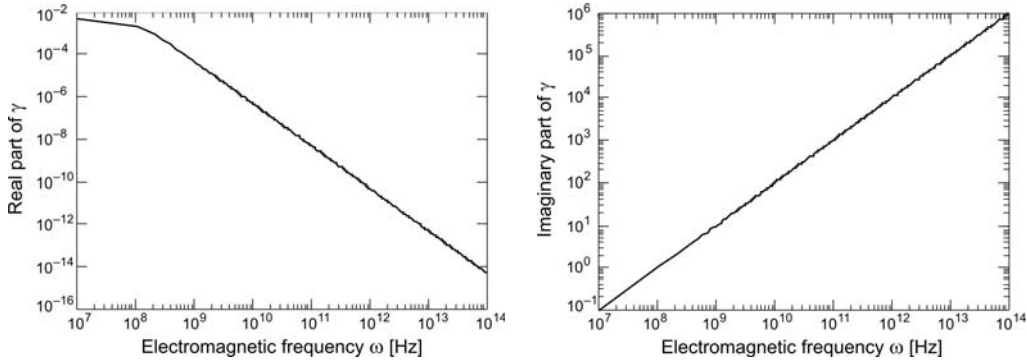


Fig. 6. Relation between transmission constant and electromagnetic frequency.

So, the power absorbed by plasma is

$$P_a = P_0 - P_t \tag{28}$$

The relation between transmission constant $\tilde{\gamma}$ and electromagnetic frequency ω could be obtained using Eqs. (22) and (27), which is shown in Fig. 6. It can be seen that the real part of transmission constant $\tilde{\gamma}$ decreases fast with an increase of electromagnetic frequency, which is about 10^{-14} at the frequency of 10^{14} Hz. According to Eq. (27), there is nearly no attenuation of laser signal through plasma.

What is worthy of attention is that the resonance [11] of electromagnetic wave and plasma was mentioned in literature. When the frequency of electromagnetic wave is around the plasma frequency, the resonance of electrons in plasma would be enhanced. There is some peak value of absorption coefficient. When collision frequency, frequency of electromagnetic wave and plasma frequency are getting close to each other, two kinds of resonances happen instantaneously, the peak value is higher. In

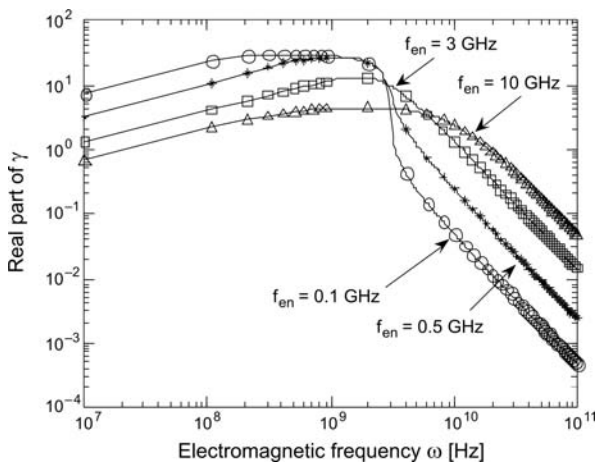


Fig. 7. Relation between attenuation coefficient and electromagnetic frequency.

order to illustrate this phenomenon, the plasma frequency was selected as 3×10^9 Hz. The relation between attenuation coefficient and electromagnetic frequency is shown in Fig. 7. Obviously, there is a peak value of attenuation coefficient at 3×10^9 Hz, and it increases with collision frequency. Certainly the above situation only occurs at the lower frequency of electromagnetic wave, for laser signal it will not happen.

3.3. Charging and discharging effects

The effects of plasma on laser signal transmission in satellite optical communication system have been analyzed, and it has been proved that the plasma imposed no obvious attenuation on laser signal. But we cannot say that the plasma has little influence on satellite optical communication system. The charging and discharging process induced by plasma occurred on the satellite surface and inner system, which is also the reason for the satellite malfunction. A schematic diagram of charging process is shown in Figure 8.

In order to analyze the charging process induced by plasma, the satellite surface is divided into several equivalent planes. The resistor of the i -th unit is denoted by R_i , capacitance by C_i , the electricity flown in by I_{T_i} , voltage by φ_i , the resistance of metal unit is denoted by R_0 , capacitance by C_0 , the electricity flown in by I_{T_0} , voltage by φ_0 ; φ_i and φ_0 satisfy [12]

$$\left\{ \begin{array}{l} \frac{d\varphi_1}{dt} = \frac{\sum_{i=0}^n I_{T_i}}{C_0} + \frac{I_{T_1}}{C_1} - \frac{\varphi_1 - \varphi_0}{R_1 C_1} \\ \dots \\ \frac{d\varphi_n}{dt} = \frac{\sum_{i=0}^n I_{T_i}}{C_0} + \frac{I_{T_n}}{C_n} - \frac{\varphi_n - \varphi_0}{R_n C_n} \\ \frac{d\varphi_0}{dt} = \frac{\sum_{i=0}^n I_{T_i}}{C_0} \end{array} \right. \quad (29)$$

The back scattering electricity is neglected, the surface electricity of the i -th unit [13] is

$$I_{T_i} = \left[J_{p_0}(1 + f_{p_D}) + J_{e_0}(f_{e_D} - 1)e^{\varphi_i/T_e} \right] A_i \quad (30)$$

$$I_{T_0} = \left[J_{p_0}(1 + f_{p_M}) + J_{e_0}(f_{e_M} - 1) \left(1 - \frac{\varphi_0}{T_e} \right) e^{\varphi_0/T_e} \right] A_0 \quad (31)$$

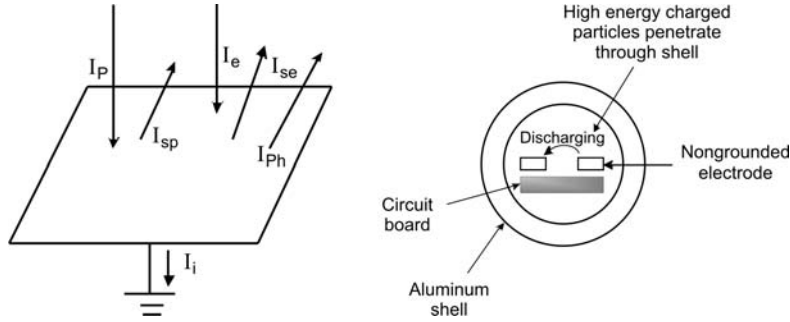


Fig. 8. Schematic diagram of surface and inner charging/discharging process.

J_{p_0} and J_{e_0} are the average electricity densities of incident ion and electrons.

$$J_{k_0} = 2.7 \times 10^{-14} n_k T_k^{1/2}, \quad k = p, e \tag{32}$$

f_{e_D} and f_{p_D} are the second radiation coefficients of nonmetal material; f_{e_M} and f_{p_M} are the second radiation coefficients of metal material; A_i and A_0 are the surface areas of the i -th unit and metal unit; T_e is electron temperature. Equation (29) can be solved by the Runge–Kuta method, the surface charging voltage of any unit can be solved by ODE23 order in MATLAB.

The second radiation electricity of electron [14] is

$$I_{T_{i2}} = J_{e_0} A_i e^{\phi_i/T_e} f_{e_D} = I_{T_{i1}} f_{e_D} \tag{33}$$

Based on Eq. (29), the charging processes of satellite surface of 100 and 300 eV plasma are shown in Figs. 9 and 10. The 100 eV plasma would impose no obvious charging process on satellite surface. But the 300 eV plasma would cause the charging

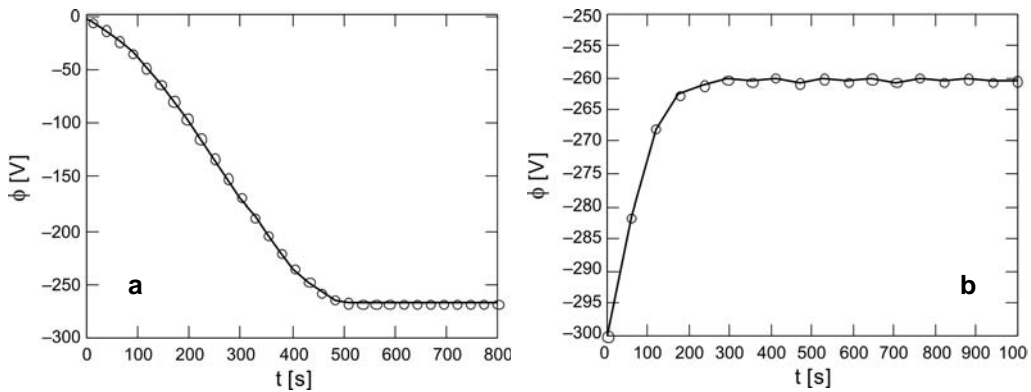


Fig. 9. Surface charging process of 100 eV plasma: initial voltage 0 V (a), initial voltage –300 V (b).

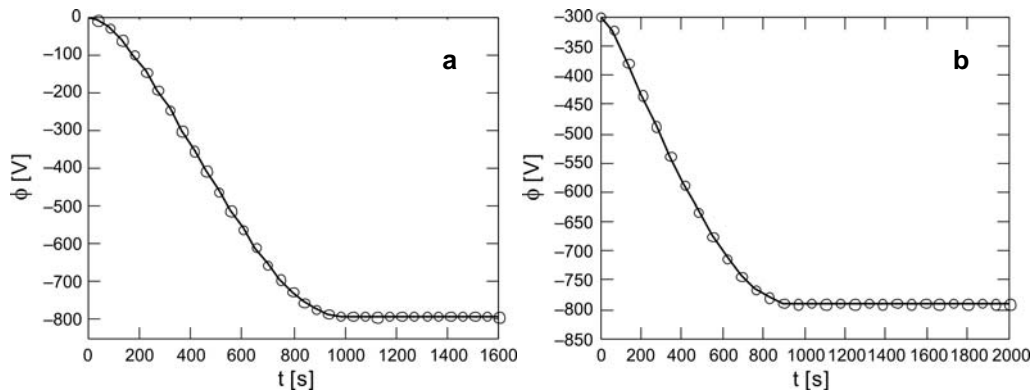


Fig. 10. Surface charging process of 300 eV plasma: initial voltage 0 V (a), initial voltage -300 V (b).

voltage of satellite surface to get close to -800 V, which would cause arc discharging. It has been proved that the middle energy plasma like 300 eV could effectively disturb the normal functions of satellite optical communication system.

4. Conclusions

Nearly 40% of satellite malfunctions were induced by space environment, mainly including high energy charged particles, solar radiation, plasma environment and space fragment. The charged particles are common in space, which might cause single event upset and total dose effect. This is also related to plasma in space. For SEU analysis the relation between single proton upset rate and satellite orbit has been analyzed in detail. The reliability index of equipment based on SEU has been proposed, the numerical calculation results have proved the SEU effect to be relatively less and correspond to higher reliability of SRAM/MOS equipment under lower orbit altitude and inclination. For plasma environment analysis there is no obvious influence of plasma on laser signal transmission, but charging and discharging processes on satellite surface would lead to the malfunctions of satellite communication system. Although research into satellite optical communication system has been carried out for many years, there is scarce literature to comprehensively analyze the influence of space environment on satellite optical communication system, which would be helpful for the design and the performance and stability of satellite optical communication system. The charged particles and related plasma are first investigated, other space environments like solar radiation, temperature variation and space fragment need to be further investigated.

Acknowledgements – This work was supported by the National High Technology Research and Development Project of China (863); (Grant No.2007AA01Z294).

References

- [1] ZHAO SHANG-HONG, *Optical communication system*, Xi Dian University Publishing Company, 2005 (in Chinese).
- [2] HOU RUI, ZHAO SHANG-HONG, LI YONG-JUN, *et al.*, *Analysis of space environment effects on satellite optical communication system*, *Optical Communication Technique* **32**(4), 2008, pp. 61–63.
- [3] YU QINGKUI, ZHAO DAPENG, *SEU rate prediction induced by space particles*, *Chinese Space Scientific Technology* **53**(6), 1998, pp. 56–61.
- [4] XUE YUXIONG, CAO ZHOU, *SEU rate calculation induced by high energy proton on satellite based electronic system*, *Space Craft Environmental Engineering* **22**(8), 2005, pp. 192–195.
- [5] PETERSEN E.L., *The SEU figure of merit and proton upset rate calculations*, *IEEE Transactions on Nuclear Science* **45**(6), 1998, pp. 2550–2562.
- [6] PETERSEN E.L., *Predictions and observations of SEU rates in space*, *IEEE Transactions on Nuclear Science* **44**(6), 1997, pp. 2174–2187.
- [7] BARAK J., REED R.A., LABEL K.A., *On the figure of merit model for SEU rate calculations*, *IEEE Transactions on Nuclear Science* **46**(6), 1999, pp. 1504–1510.
- [8] GARRETT H.B., WHITTLESEY A.C., *Spacecraft charging: An update*, *IEEE Transaction on Plasma Science* **28**(6), 2000, pp. 2017–2028.
- [9] GREGDIRE D.J., *Electromagnetic Wave Propagation in Unmagnetized Plasma*, ADA250710, 1992.
- [10] SUN AIPING, LI LIQIONG, QIU XIAOMING, *Interaction of the electromagnetic waves and non-magnetized plasmas*, *Nuclear Fusion and Plasma Physics* **22**(3), 2002, pp. 135–137.
- [11] MENGU CHO, HOSODA S., OKUMURA T., *et al.*, *Intermediate report on development of high voltage solar array in LEO plasma environment*, *Radio Science Conference 2004*, pp. 612–613.
- [12] YANG JUAN, SU WEIYI, MAO GENWANG, *On calculating effectiveness of Plasma defense against low orbit spy satellite*, *Journal of Northwestern Polytechnical University* **23**(1), 2005, pp. 93–96.
- [13] GU SHIFEN, SHI LIQIN, ZANG ZHENQUN, *Arc discharges for high voltage solar array in the space plasma*, *Chinese Journal of Space Science* **15**(2), 1995, pp. 131–135.
- [14] LI JIAWEI, LI ZHONGYUAN, *Charging process of space dust and its dependence on plasma parameters*, *Chinese Journal of Space Science* **24**(5), 2004, pp. 321–323.

*Received September 23, 2008
in revised form November 23, 2008*